10-12-2018

Rates of planimetric change in a proglacial gravel-bed braided river: field measurement and physical modeling

Lara Middleton
U. Western Ontario, lmiddle7@uwo.ca

Peter Ashmore
pashmore@uwo.ca

Pauline Leduc

Darren Sjogren
University of Calgary

Earth Surface Processes and Landforms BSG British Society for Geomorphology

Rates of planimetric change in a proglacial gravel-bed braided river: field measurement and physical modeling

Journal:	*Earth Surface Processes and Landforms*
Manuscript ID	ESP-18-0147.R2
Wiley - Manuscript type:	Research Article
Date Submitted by the Author:	n/a
Complete List of Authors:	Middleton, Lara; University of Western Ontario, Geography Ashmore, Peter; University of Western Ontario, Geography Leduc, Pauline; Western University, Department of Geography Sjogren, Darren; University of Calgary, Department of Geography
Keywords:	planimetric change, bedload transport, braided river, experimental modelling

Note: The following files were submitted by the author for peer review, but cannot be converted to PDF. You must view these files (e.g. movies) online.

Middleton_Sunwapta_Video_2012.mp4
Middleton_Flume_Hydrograph_Video.mp4

Graphical Information

Rates of planimetric change in a proglacial gravel-bed braided river: field measurement and physical modeling

L. Middleton*[1], P. Ashmore[1], P. Leduc[1], D. Sjogren[2]

[1] Department of Geography, University of Western Ontario, London, Ontario, Canada, N6A5C2

*Corresponding author: lmiddle7@uwo.ca

[2] Department of Geography, University of Calgary, Calgary, Alberta, Canada

Key Points

- In a proglacial, gravel-bed, braided river the measured areas of planimetric change increases in relation to peak and total daily meltwater discharge above a threshold.
- A physical model of the field site had very similar planimetric change area and threshold discharge as the field data and showed that the threshold discharge for gravel bedload is almost the same as the planimetric change threshold.
- Morphological change and total bedload transport for a hydrograph correlate with planimetric change, and this raises the possibility that rate of planimetric change may be used as surrogate for bedload monitoring while also providing measurements of braiding dynamics over the full range of discharge.

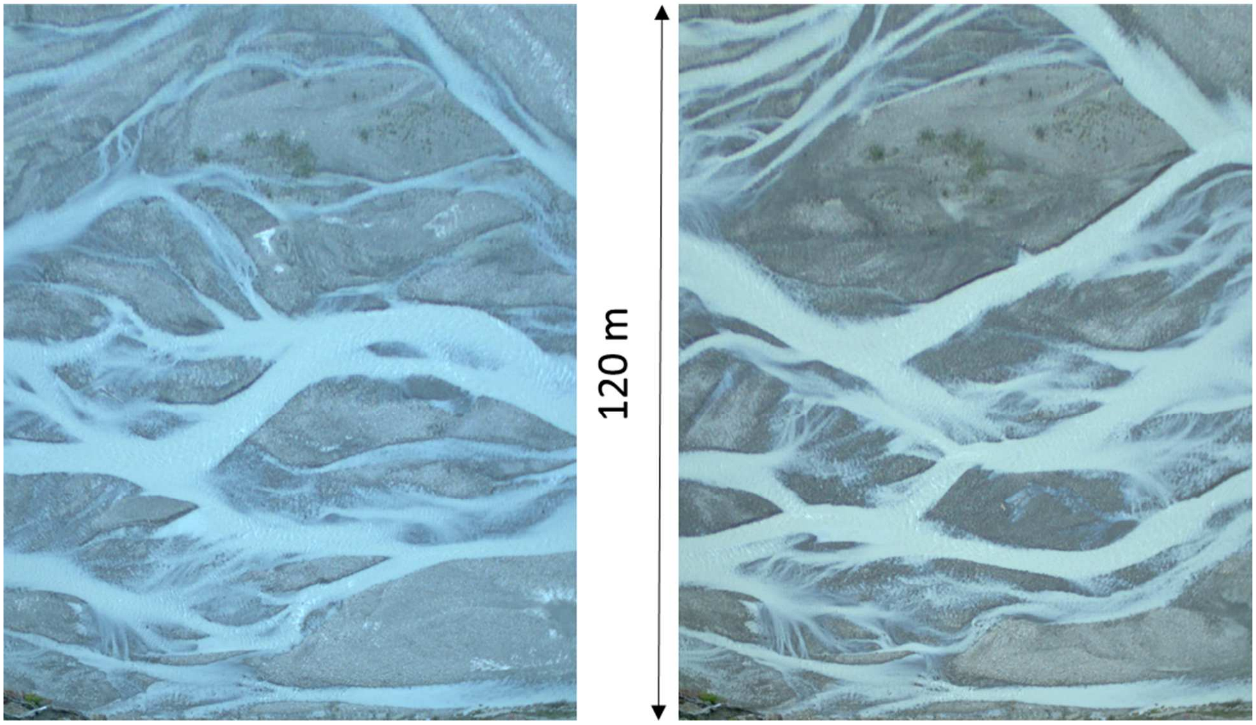

July 8, 2012, 8:00
Q: 4.00 $m^3 s^{-1}$

July 23, 2012, 7:30
Q: 3.87 $m^3 s^{-1}$

Rates of planimetric change in a proglacial gravel-bed braided river: field measurement and physical modeling

L. Middleton*[1], P. Ashmore[1], P. Leduc[1], D. Sjogren[2]

[1] Department of Geography, University of Western Ontario, London, Ontario, Canada, N6A5C2

*Corresponding author: lmiddle7@uwo.ca

[2] Department of Geography, University of Calgary, Calgary, Alberta, Canada

Short Title:

Rates of planimetric change in a braided river

Key Points

- In a proglacial, gravel-bed, braided river the measured areas of planimetric change increases in relation to peak and total daily meltwater discharge above a threshold.
- A physical model of the field site had very similar planimetric change area and threshold discharge as the field data and showed that the threshold discharge for gravel bedload is almost the same as the planimetric change threshold.
- Morphological change and total bedload transport for a hydrograph correlate with planimetric change, and this raises the possibility that rate of planimetric change may be used as surrogate for bedload monitoring while also providing measurements of braiding dynamics over the full range of discharge.

Abstract

Planimetric change was measured on daily hydrographs over two meltwater seasons using time-lapse images of the proglacial, gravel, braided, Sunwapta River, Canada. Significant planimetric change occurred on 10-15 days per year. Area of planimetric change correlated with peak and total daily meltwater hydrograph discharge. A clear threshold discharge can be identified below which no planform activity occurs, an intermediate range over which change occurs conditionally, and a peak flow range at which significant change always occurs. Field conditions were reproduced in a physical model in a laboratory flume. Photogrammetric DEMs of bed morphology and measurements of bedload output were made for each hydrograph experimental run. The physical model results for planimetric change had a threshold discharge for change, and trend with discharge, similar to the field data. The model data also show that planimetric change correlates strongly with volumes of erosion/deposition measured from successive DEMs, and with bedload transport rate. The relation between planimetric change and topographic change is also apparent from previous cross-section surveys at the field site. The results highlight the planimetric dynamics of braiding rivers in relation to discharge forcing, and the relationship between planimetric change, morphological change, and bedload transport in braided rivers. This also points to the potential use of measurements of planimetric change from time-lapse imagery as a low-cost method for high-frequency monitoring for braiding dynamics and also a surrogate for bedload transport measurement.

Keywords: braided river, planimetric change, bedload transport, experimental modelling

Introduction

Gravel-bed braided river planform is characterized by rapid reconfiguration at high discharge related to highly active unit processes of bar formation, migration and erosion, local scour, channel bifurcation and avulsion (Ashmore, 1982, 2013). While the processes of braiding have been well-described, the quantification of rates of channel planform change over a range of discharges to characterise braiding dynamics has not been quantitatively documented. Time-lapse monitoring has provided useful insights into braiding processes over a range of discharge (Hicks et al., 2000; Bertoldi et al., 2010) but planimetric changes have seldom been explored systematically. To date, studies monitoring braided planform have focussed on detailed bar-scale elements at high frequency (Arscott et al., 2002; Bertoldi et al., 2012), or more general large-scale changes at a low frequency over years/decades to document channel changes (Warburton et al., 1993; Luchi et al., 2007; East et al., 2017).

Channel changes over multiple years/decades have also been used to construct long-term sediment budgets (Martin and Church, 1995; McLean and Church, 1999; Ham and Church 2000; Gaeuman et al., 2003). These studies have mapped wandering and low-intensity braided channels over multiple year time intervals to infer bedload volumes using aerial imagery and topographic surveys. Short-term planform dynamics of gravel-bed braided rivers related to single-events have not been documented and measured in detail with repeated, systematic observations over a range of known event discharge.

Recent advances in high resolution mapping of river morphology have been applied to braiding rivers to document reach-scale volumetric sediment budgets along with information on planform dynamics and extended to estimates of bedload transport rate and its spatio-temporal variation (Ashmore and Church, 1998; Bertoldi et al., 2010; Wheaton et al., 2013; Williams et al., 2015; Mao et al., 2017; Vericat et al., 2017). These data sets are beginning to form a basis for analysis of braided river morphodynamics and for computational model development (Ziliani et al., 2013; Williams et al., 2013, 2016; Javernick et al., 2014, 2016). However, hyper-resolution mapping of full topographic change in a braided river reach remains a time-consuming and technically challenging exercise (Vericat et al., 2017) and data sets are still limited in number and temporal frequency.

The studies of morphological change and reach-scale budgets demonstrate the close association of these processes with the local bedload flux. This provides an alternative to direct measurement or prediction of braided river bedload transport rate that has long been problematic (Recking et al., 2016). Davies (1987, p. 794) encapsulated the problem by describing braided river channels as a varying number of single channels, each with its own high degree of variability in geometry and bedload transport rate, and each with a flow rate that is an interdependent and time-varying proportion of the total river flow. Davies (1987) suggested that planimetric properties of braided channels are an easily measured and monitored aspect of braided river morphology, and that bedload may correlate with planform configuration and dynamics. Braided channels are laterally unstable and mobile, and this lateral mobility makes morphological change and associated bedload transport detectable as a planimetric change. This idea seems not to have been systematically pursued over a short temporal frame in braided rivers. Some previous studies have found qualitatively that temporal fluctuations in bedload relate to particular morphological processes such as bar migration and planform switching, that are expected to have clear planimetric signals, especially in braided rivers (Ashmore, 1991; Hoey and Sutherland, 1991; Bertoldi et al., 2009). This shows a possible association between planform change, morphologic change, and bedload flux in a gravel-bed braided river. Planimetric changes may be monitored much more easily than bed topography, even with the new technologies available for the latter. Therefore, Davies' proposition that planimetric change may be useful surrogate for bedload transport measurement is worth pursuing in more detail and doing so would, in the process, build observations on braided river planform processes and rates of change dynamics over a range of discharge. Understanding the intrinsic relationships among discharge and planform change and extending them to topographic change and bedload would help further understanding of braiding morphodynamics.

Gravel-bed braided rivers are common in proglacial environments and some of the existing understanding of braided river morphodynamics and bedload comes from such rivers (Goff and Ashmore 1994; Meunier et al., 2006; Liu et al., 2007). The regular diurnal hydrographs of proglacial rivers provide frequent bed mobilizing events during summer meltwater periods. This provides a useful setting for natural experimental investigation of braided river planform dynamics in general, and in relation to proglacial flow regimes in particular. In this paper we investigate planform dynamics in a proglacial gravel-bed braided river using high frequency (half-hour) field monitoring of planform dynamics and discharge. We connect planform dynamics to morphological change (following usage of Williams et al. (2012) we use 'morphological change' to refer to the full 3D river bed dynamics and the associated morphological units) and bedload by extending the study using physical modeling of representative hydrographs from the field site in a laboratory river tray. The field monitoring had three objectives: 1. develop a relationship between rate of planimetric change and discharge over many daily hydrographs in a proglacial gravel braided river; 2. assess the frequency and time sequence of planimetric change during two, summer meltwater seasons, and 3. compare the extent of planimetric change (active width) at the field site with measurements of topographic active width from previous studies at the same site (Ashmore et al., 2011).

In the physical model, morphological change and bedload transport data were acquired that could not be collected at a daily frequency, over an extended period in the field setting. The physical experiments were run to extend our inquiry to three further objectives: 4. compare areas of planimetric change between field and model settings and assess the possible discrepancy between planimetric change and the areas and volumes of erosion and deposition measured from high resolution DEMs of the model; 5. assess whether planimetric change correlates with bedload transport rate and if there is any significant 'background' bedload flux occurring in the absence of planimetric and morphological change and consequently 6. assess the potential for using planimetric change as a surrogate for bedload transport rate in field monitoring of gravel-bed braiding rivers.

Data Collection

Field Site

Field data were collected on the Sunwapta River in Jasper National Park, Alberta, Canada. At the study site, the Sunwapta River is a small (approximately 120 m overall river width) proglacial, gravel-bed braided river with a braiding intensity of 3-5 at morphologically active discharges. The Sunwapta originates at the outlet of Sunwapta Lake, draining the Athabasca Glacier (Figure 1). The study reach has a surface grain size D_{50} of 41 mm and D_{90} of 85 mm. The surface and subsurface grain size distributions are very similar based on 19 aggregated surface and subsurface samples (truncated at 8 mm) taken across the river with 2500 stones in the surface sample and bulk subsurface sample with total mass of approximately 1500 kg. River gradient is approximately 1.5% (Chew and Ashmore, 2001). Previous studies at this site beginning in the early 1990s (Goff and Ashmore, 1994; Chew and Ashmore, 2001; Chandler et al., 2002; Ashmore and Sauks, 2006; Ashmore et al., 2011) provide background on the river morphology and comparative data on river topography, hydraulic geometry, channel planform processes, and morphodynamics.

The bulk of the annual flow, and the annual maximum flows, of Sunwapta River occur during the summer melt-water period from late June to early September. The overall channel planform and bed topography change over this time period, especially during peak flow periods in July and August based on repeat daily cross-section re-surveys and daily imagery for periods of 10-20 days in 1989, 1993, 1999 and 2003 (Goff and Ashmore, 1994; Ashmore et al., 2011).

Study Reach Discharge

Planimetric change was measured throughout the summer meltwater season from June to September 2012 and 2013. The diurnal ice and snow melt cycle during this period produces a consistent daily hydrograph repeated on a regular cycle each with a 24-hour time base. Individual daily hydrographs could therefore be viewed as separate flow events, each capable of producing planimetric change. Observed flows during 2012 and

2013 were representative of the typical summer melt-water flows on record for the Sunwapta River, dating back to 1948 (Figure 2a), and cover the full range of discharge in the river. The regular diurnal discharge cycles are superimposed on longer period (multiple days) phases of higher and lower flows related to synoptic weather events during the summer (Figure 2a).

The Water Survey of Canada (WSC) operates a gauging station (07AA007) at the outlet of Sunwapta Lake (Figure 1), which provided a continuous stage and discharge record at 15-minute intervals, seasonally from May – October. The braided study reach receives an additional input of flow from the Dome Glacier meltwater stream (Figure 1), which is not accounted for in the WSC gauge record. To account for the additional input, a total of 175 discharge measurements collected downstream of the Dome confluence were correlated with WSC discharge. Discharge was measured through velocity-area gauging, conducted in the meltwater seasons of 2015 and 2016 using flow meters at a confined section of the study reach and at the Dome Glacier meltwater stream. Additionally, a time-lapse camera was installed to monitor the Dome Glacier melt-water stream during the entire melt-water season of 2015. Timing of flow variation over both a diurnal and weekly temporal scale coincides between the Dome melt-water stream and Sunwapta River (Leduc et al., 2017). Using the discharge analysis of Ashmore and Sauks (2006) for this site, and additional discharge measurements from 2015 and 2016, the rating curve from the combined data gives a continuous discharge record (± 0.50 $m^3 s^{-1}$) for the summer meltwater season (Figure 2b).

Time-Lapse Image Collection

Time-lapse images were taken with a Reconyx Hyperfire 650 camera, installed on a cliff ledge approximately 90 m above and 190 m horizontally away from the middle of the river bed (Figure 1). This camera location and geometry gave images covering the full width of the river and channel length of about 100 m on the river bank closest to the camera. The camera was programmed to take a picture every 30 minutes beginning at 0600 hours and ending at 2200 hours each day, capturing the daily minimum and peak flow (which occur at approximately 08:00 and 19:00 respectively), but portions of the falling stage occurred at night. The high frequency of images allowed the river planform to be captured at a comparable stage on successive days.

Planform Measurement

Analysis of images was used to produce daily planimetric change measurements for each daily hydrograph. Each diurnal discharge cycle was analyzed as an individual flow event. It was apparent that any planform change occurred over a limited time each day and not during the daily low flow, even during the highest flow periods. Therefore, these diurnal hydrographs are separate planform change events.

The oblique images were ortho-rectified using ten ground control targets, visible in the initial photographs for each year, surveyed with high-precision dGPS (cm-dm, Model: Trimble R8, Real-time Kinematic surveying, CGG2013, NAD83 [CSRS], Orthometric Heights). The number of pixels between each of the target points in an oblique photograph was used to derive a pixel-meter (distance) relationship for the entire image. Distances between each of the ten ground control points in the rectified images and ground distances (45 measurements) are strongly correlated (R^2: 0.99), with a standard error of estimate of 0.014 m.

Planimetric change measurement for a given diurnal hydrograph was based on selecting pairs of photographs on successive days at the lowest recorded comparable discharge during the morning low flow period. Using images at low flows minimized apparent effects of stage differences (which could mask real planform changes) and maximized the area of river bed visible for planform mapping. Five day-to-day comparisons with no similar discharge on the two days were removed from analysis. Visual assessment and measurement of daily planimetric changes gave rates of planimetric change and information on typical processes of change: lateral and mid-channel bar formation, accretion, migration and erosion; bank retreat and accretion; and channel avulsion and migration. A 96 x 120 m grid, with 6 x 6m grid squares superimposed on the rectified images aided in digitizing visible changes in the river planform. Individual polygons of planimetric change were mapped using ImageJ software (Schneider et al. 2012) and summed to determine the total area of planimetric change. Repeat measurements from 20 diurnal hydrographs to check reliability and precision had a high degree of similarity between the original and re-measured areas of change (R^2: 0.90, with a standard error of estimate of 0.019 m^2).

Peak daily discharge is used in the analysis of planimetric change. Some previous work on event scale morphological change has used total flow volume. (Haschenburger, 2013; Wheaton et al., 2013; Papangelakis and Hassan, 2016) but the daily meltwater hydrographs all have a similar shape and time base, and consequently peak discharge and total discharge are strongly correlated (R^2: 0.94 and 0.91 for the two years, with a

226 standard error of estimate of 0.016 $m^3 s^{-1}$ and 0.029 $m^3 s^{-1}$). The maximum daily
227 discharge is therefore a measure of peak stream power and a reliable indicator of total
228 daily energy expenditure driving channel planform change.

229 Time-lapse imagery allowed changes in the river planform to be documented
230 continuously throughout the meltwater season, across the full range of known flows. As
231 an example of the raw image series and planform dynamics, see the supplementary
232 information for this paper showing a time-lapse video of a 15 day flow period on the
233 Sunwapta River from July 7-22, 2012. Time and date are in the top, right hand corner of
234 the video.

235 **Physical Model**

236 The model experiments were completed after the collection and analysis of the field
237 data using a river-modelling flume and based on a Froude-scaled physical model with a
238 length scale of approximately 1:33 of the Sunwapta River reach, based on geometric
239 scaling of the grain size distribution. Froude-scale modelling is used in gravel-bed
240 braided river research to preserve geometric and dynamic similarity in the model
241 relative to the full-scale river (Ashmore and Parker, 1983; Ashmore, 1988; Young and
242 Davies, 1990; Hoey and Sutherland, 1991). In particular non-dimensional bed shear
243 stress is the same in model and full scale river which preserves bed particle mobility
244 and related morphodynamic processes (Ashmore, 1982; Peakall et al., 1996; Young
245 and Warburton, 1996; McKenna Neuman et al., 2013; Redolfi et al., 2016). The lower
246 limit of the grain size distribution was truncated so that grains smaller than 0.18 mm
247 (equivalent to approximately 8 mm in the field) were excluded because the scaled-down
248 portions of the finer field grain sizes may affect bedform and dynamic similarity of the

model (Young and Warburton, 1996; McKenna Neuman et al., 2013). The median grain size of the flume sand was 1.18 mm and the D_{10} and D_{90} were 0.32 mm and 3.52 mm respectively. The model dimensions were 18.3 x 3 m with the gradient set to 1.5%, equivalent to the slope at the study reach. The initial channel configuration was a single, straight, channel from which a braided morphology self-formed under a constant discharge (see also Peirce et al., 2018). A series of 3 different hydrograph experiments, each with a peak of 2.1 l s^{-1}, were run prior to the hydrographs described in this paper. The model is not an exact replica of the channel pattern in the field at any particular time (which varies in any case) but is expected to give braiding morphology and dynamics that model the characteristics of the field site.

The scaled model hydrographs reproduced daily hydrographs from the Sunwapta River, with peak discharges above the threshold for planimetric change. A sequence of four daily hydrographs with different peak discharges was run three times, for a total of 12 hydrograph experimental runs (Figure 3). The 1:33 Froude-scaled model yields a discharge scale of 1:6250 giving peak discharges of the four hydrograph experiments of 1.3, 1.6, 2.2 and 2.9 l s^{-1}, equivalent to a peak of 8, 10, 14, and 18 m^3 s^{-1} respectively, on the Sunwapta. The time base of the hydrographs assumes a Froude time scale of the square root of the length scale. Bedload output at the downstream end was continuously recirculated to the upstream end of the model river, maintaining an overall sediment balance during each experimental run.

Planform Measurement

Planform and bed topography were surveyed using two digital SLR cameras mounted on a trolley on the rails about 2.9 m above the flume. The convergent geometry of the cameras across the flume on either side of the trolley gave ~80 % lateral overlap between images from the two cameras. Surveys of the whole flume used a longitudinal overlap of 60% resulting in an average of 100 photos (50 from each camera) to cover the entire length of the flume with a pixel resolution of approximately 1 mm on the model river bed. Planimetric measurements used a stitched orthomosaic of a 9.5 x 3 m area of the model river processed in Agisoft Photoscan 1.0.0.1 Standard (Version 1.2.6) (Software) (2016*) during the rising and falling stage, and peak discharge of each hydrograph. Measurement of the area of planimetric change used a method equivalent to that used in the field images.

During experimental runs, time-lapse images were also taken with two Olympus C5060 cameras with wide angle lenses, located in a fixed position 3 m vertically above the central axis of the flume and 6m apart. These images provided a high frequency (1 minute) time lapse record of each experiment which is included in the supplementary information for this paper.

Morphological Measurement

Agisoft PhotoScan was also used to generate DEMs from images of the drained bed at the beginning and end of each hydrograph (Kasprak et al., 2015; Morgan et al., 2016; Peirce et al., 2018). DEMs of Difference (DoD) of successive DEMs gave measurements of areas and volumes of morphologic change during each hydrograph. DoD processing began with application of a simple threshold with all elevation change values less than the threshold (3σ) removed. Application of a dilation filter modified the simple threshold map by reducing noise and increasing continuity between areas of change. The dilation filter used a binary mask from the threshold analysis to include

295 areas of change of less than 3σ that are within a radius of 15 cells (22.5mm) (based on
296 trials with different radii) adjacent to change areas above the threshold (see also Peirce
297 et al., 2018).

298 *Bedload Transport Measurement*

299 Bedload samples were collected in five baskets at the downstream end of the flume,
300 accumulating sediment for one minute at each hydrograph step, for a total of 141
301 samples. Samples were dried, weighed and sieved to obtain bedload transport rates
302 and particle size distributions of bedload. The total bedload weight transported during a
303 hydrograph was calculated by multiplying the weight from each one-minute sample over
304 the total time at the hydrograph stage and summed over the hydrograph.

305 **Results**

306 **Field Data, Sunwapta River**

307 Daily peak discharges ranged from under 1.5 $m^3\ s^{-1}$ to over 21 $m^3\ s^{-1}$, covering the full
308 range of observed historical meltwater peaks on the river. Measurable and variable
309 planform change occurred on multiple days each year (Figure 4). Of the 216 daily
310 planimetric measurements made in the two years (113 in 2012 and 103 in 2013), 158
311 daily hydrographs showed no observable planimetric change. In both years the most
312 pronounced areas of planimetric change were activated in the first high flow period of
313 the season in early to mid-July, even though equivalent flows also occurred later in the
314 season (Figure 4). Planimetric change tended to occur in groups of sequential days
315 (typically between 5-7) all having daily high flows near the upper range for the season.
316 The bulk of significant planform change occurred on those 10-15 days each year
317 (Figure 4).

Measured areas of daily planform change increased in relation to discharge above a daily peak discharge of approximately 11 $m^3 s^{-1}$ (Figure 5). Less than 10% (10 days total) in which peak flow was 11 m^3s^{-1} or lower showed any observable change and these were all very minor, with a maximum area of change, less than 1% (80 m^2) of the wetted area of the channel.

Above a peak daily flow of 11 $m^3 s^{-1}$ planimetric change increased with increasing discharge (Figure 5). For hydrographs with daily peak discharge between 11 and 17 $m^3 s^{-1}$ occurrence of planimetric change was inconsistent, with extensive areas of planform change on some days but none on others. Daily peaks exceeding 17 $m^3 s^{-1}$ always produced large areas of planform change but the total area of change was variable (Figure 5).

The scatter in the relationship between planimetric change and-discharge may be partly the result of secular variability within groups of days. Planimetric change tends to be more pronounced during the initial two or three days of rising flow sequences, and also high flows near the beginning of the meltwater season appear to produce more planform change than equivalent flows later in the season (Figure 4). Planimetric change therefore seems to be partly contingent on timing and the braiding pattern changes rapidly during initial high flow phases but then settles into a more stable phase. This also partly reflects the inherent variability in braiding dynamics in which temporal variability in process rates occur even under experimental constant-forcing discharge (Ashmore, 2013).

The style of planimetric change differs with discharge conditions. Planimetric changes below a daily peak of 14 $m^3 s^{-1}$ were minor; primarily small areas of bar and bank erosion potentially leading to the local lateral migration of the channel or minor modification to bars (Figure 6a). Above 14 $m^3 s^{-1}$, larger scale changes in river planform occur, including planform shifting across the entire river width from channel avulsion, confluence migration, channel expansion and migration, and large areas of bar erosion and deposition (Figure 6b). This is clearly seen in the time-lapse video from the field site in the Supplementary Material.

The use of time-lapse imagery in the field made it possible to analyze the entire four-month meltwater flow season. Measurements of planimetric change and areas of change from this study could then be compared with previous surveys of topographic change at this site. Cross-section surveys done in 1999 and 2003 at this site allowed a comparison between daily topographic change and areas of planimetric change at different discharges. The previous topographic measurements consist of 10-12 repeat cross-sections per day in the same reach as the time-lapse planimetric changes reported above (Ashmore et al., 2011). The active width (lateral extent of bed elevation change) was measured for each daily hydrograph over 2-3-week periods in 1999 and 2003. Areas of planform change were made non-dimensional using the average wetted width at the daily peak. Dimensionless stream power ($\omega*$) was used to develop a potential universal relationship across different scales and types of braided rivers. Dimensionless stream power was calculated as defined by Bertoldi et al. (2009):

$$\omega^* = \frac{QS}{b\sqrt{g\Delta D_{50}^3}} \qquad \text{(Eq1)}$$

where Q is the discharge, S is the slope, b is the average wetted width, g is the acceleration due to gravity and D_{50} is the median grain size.

The results show a threshold dimensionless stream power for active width, and variability in the correspondence between planimetric and cross-section topographic change (Figure 7). In both cases, there is variability around the relatively small range of dimensionless stream power, and the planimetric data extend the existing relationship to lower stream power while showing a slightly lower threshold condition compared to the topographic change. This is possibly related to a higher change detection threshold in the topographic surveys.

Physical Model Results

The model data cover the full width of the river and a length equivalent to 2.7 times that in the field images. To compare how representative the shorter reach measurements in the field are relative to the longer reach possible in the lab, planimetric measurements were also made over three smaller blocks, equivalent to the reach length in the flume. Measurements were scaled by the reach length to provide a metric independent of reach length.

The physical model results are closely comparable with the field data when scaled (Figure 8). Hydrographs with peak discharges of 1.6 l s^{-1} (equivalent to 10 $m^3 s^{-1}$) and less showed very limited planimetric change (less than 5% of the total surveyed area) in the model, so that the range of threshold discharge for detectable planimetric change was very similar to that in the field. Types of planform changes were similar in character to those observed in the field, being mainly minor isolated areas of bank or bar erosion along the primary channel. The hydrograph experiments with a peak discharge of 2.22 l s^{-1} (equivalent to 14 $m^3 s^{-1}$) and higher produced larger areas of planimetric change. As in the field results, these changes occurred across the entire length and width of the river area. The model results tend to be at the higher end of the range of planform measurements observed and one reason may be that the clear water in the model allowed identification of change areas that would be submerged by the turbid water in the field. The greatest difference is seen in the range of 11-16 $m^3 s^{-1}$ (Figure 8) where no planimetric change occurs in some cases but not in the smaller sample size in the model experiments in this discharge range.

Bedload Transport Rates vs Planform and Morphological Change

Total bedload transport mass for a hydrograph event increases with peak discharge (Figure 9a) with a threshold discharge for bedload transport similar to that for the planimetric change. The result shows that there is negligible bedload transport for the gravel size fraction independent of measurable planimetric change. Consequently, there is also a close correlation between the area of planform change and bedload transport rate (or mass) for a hydrograph (Figure 9b, c). Planimetric change alone therefore may be a reliable approximation of bedload transport for an event hydrograph. This relationship may be modified however, in circumstances when the main channel is confined against the flume wall (or equivalent condition in the field) and the erosion-deposition exchange of active braiding is modified by pronounced local scour. This was the case for the two highest points on Figure 9b so that the planform-bedload relationship, including the bedload discharge threshold, appears to change in these circumstances.

Volumes of morphological change (from DEMs of difference) and bedload transport showed a threshold discharge of ~1.6 $l\ s^{-1}$ (equivalent to 10 $m^3 s^{-1}$) similar to that of planimetric change, below which morphological change and bedload flux were negligible. Volumes of morphological change and the total bedload transport mass both were found to have a positive, significant relationship with simultaneous measurements of the area of planform change (Table 1).

Total volume of morphological change also shows a strong correlation with peak hydrograph discharge and threshold discharge, similar to that for the planimetric change and bedload (Figure 10a). The areas of morphological change measured from DEMs of Difference for each hydrograph (Figure 10b) show coherent spatial patterns that are distributed over the entire channel area along the main anabranches of the braided channel. As peak hydrograph discharge increases (Figure 10b), the few small scattered areas of change apparent only along the main channel at low peak discharge (Runs 4 and 5, Figure 10b), expand along the main channel, with areas of alternating erosion and deposition. At the two higher peak discharges the areas of change also expand laterally, enlarge (reflecting larger scale bar and bank erosion), become more continuous along the channel, and activate secondary channels in the braided network as full active braiding begins to occur in the entire channel.

The extent and spatial pattern of areas of change measured from planimetry and DEMs of Difference correlate closely, as do areas and volumes of change (Figure 11). However, there are some differences in detection of planimetric and morphological change, such that planimetric changes tend to be underestimated relative to change areas from the DEMs of Difference. The planimetric measurements underestimate the area of change from a DoD by an approximate factor of 2, even though they are well correlated (Figure 11b). A major source of difference appears to be that the DoD area included areas of erosion and deposition along the channel bed, under the water surface that do not appear as obvious planimetric shifts in the orthoimages from which planimetric change was measured.

One approach to using planimetric (or morphologic) change data to estimate bedload in braided rivers is to combine the mass of material mobilized with the path length (distance of movement from erosion to deposition site during a transporting event) to derive an event bedload transport rate (Ashmore and Church, 1998; Church 2006; Kasprak et al., 2015, Mao et al., 2017). Path length is usually assessed using tracer particles, but data and general predictions of path length are sparse. An alternative to direct tracing of particles is to invert the bedload equation to yield the path length necessary for the known relation between mobilized sediment mass and bedload transport rate. With a known bedload transport rate, and volume of erosion, the equation can be rearranged to determine estimates of the path length:

$$Lt = Q_b \, \alpha / Ve \qquad \text{(Eq2)}$$

Where Lt is the estimated path length (m), Q_b is the known transport rate (g/min), α is the reach length multiplied by time (m*min) and Ve is the volume of erosion (m^3). Figure 12 shows this path length value for the hydrographs from the physical model. The range of path lengths is similar for each of the three lowest hydrographs of 0.5–2 m but is higher (3-5 m) for the highest peak discharge at which morphological and planimetric change is most extensive. The higher values are similar to the length of the largest braid bars in the physical model braided channel and this supports the idea that under active braiding path length may be similar to bar spacing (Pyrce and Ashmore, 2003; Church, 2006; Hundey and Ashmore, 2009; Kasprak et al., 2015).

Particle size analyses for the bedload samples also allows an assessment of particle mobility at different transport rates and planimetric change rates. Bedload transport was concentrated during the highest flow periods within each hydrograph (as was planimetric and morphological change) and was markedly higher in the three hydrographs with the highest peak flow (C) (Figure 13a). The exception was the final hydrograph at the lowest peak (D), during which the channel scoured deeply against the flume wall close to the flume outlet and produced substantial bedload locally at the outlet (see above). The median grain size of individual bedload samples showed no clear trend in relation to discharge or the mass of bedload transported but shows a slight tendency to increase at peak flow and higher transport rate (Figure 13a, lowest panel and 13b) and matches the D_{50} of the bed material in the model (i.e. full mobility). The D_{90} showed clearer trends with an increase during the peak flow phases (Figure 13a, lower panel) and with larger sample mass (transport rate) (Figure 13b) increasing from 1.5 mm to almost 4 mm between the lowest and highest discharges and transport rates. At the highest transport rate, D_{90} is very close to that of the bulk size distribution of the bed material, so that this coarse fraction is also at or close to full mobility during the most active planimetric change periods (see Mueller and Pitlick, 2014; Peirce et al., in press).

Discussion

The results demonstrate, using high frequency time-lapse imagery over two years, that the rate of planimetric change in a proglacial gravel-bed braided river increased progressively with peak (and total) diurnal hydrograph discharge. A distinct threshold of peak daily discharge is apparent below which planimetric change was negligible.

Physical model experiments reproducing a sequence of hydrographs from the field site showed the same relationship between planimetric change and discharge, including a very similar threshold for detectable change. Threshold discharge for bed elevation change mapped from photogrammetric DEMs, and the bedload transport rate in the model is very similar to the threshold discharge of planimetric change. There may be small areas of bed erosion-deposition that are not detectable in planimetric mapping. The results from this study provide a larger data set, and experimental data, supporting the study of Bertoldi et al. (2010) showing associations between discharge, planform change, topographic change, and relative bedload flux in the gravel-bed, braided Tagliamento River, Italy.

Bertoldi et al. (2010) identified two different scales of planform and morphological change associated with low and high discharge events on the Tagliamento River. Small amounts of localized bank erosion and bar deposition, primarily in the main channels, occurred during events with small amounts of morphological change. Much larger events triggered river-wide planform reconfiguration through avulsion and major bar shifts. The study of Hicks et al. (2002) also noted two different scales of planimetric and morphological change associated with bankfull floods and the following reworking by smaller floods on the Waimakariri River, New Zealand. Time-lapse imagery, taken every 20 minutes, was used to continuously monitor planform dynamics, highlighting the difference between large-scale changes and transport of large gravel sheets at high floods, and smaller changes within the channel as the flow receded and during smaller flow events. The Tagliamento River and the Waimakariri River are larger-scale braided rivers (braid plains are 1.5 km and 1 km wide respectively) and experience a different flow regime, dominated by larger rainfall floods (highest peaks analyzed: ~ 1700 $m^3 s^{-1}$ and 840 $m^3 s^{-1}$ respectively). Our results suggest a similar change in planform processes between lower magnitude and higher magnitude events, but the data on planimetric change indicate no clear break in rates of planform change across a range of discharge above the threshold discharge for initiating planimetric change.

The results add considerably to previous attempts to study discharge-related changes in braided river planform and bed morphology and extend the results to demonstrating the relationship between planimetric change and bedload transport rate. This supports Davies' (1987) proposition that a relationship might exist between bedload transport and planimetry of braided rivers. The outcome is also consistent with expectation from previous work that bedload transport can be estimated in gravel braided rivers (and other gravel-bed river morphologies) using morphological change (Ashmore and Church 1998; Church, 2006; Vericat et al., 2017) but importantly demonstrates that planimetric change alone may give reliable estimates of bedload along with analysis of processes, patterns, and rates, and their spatio-temporal variation. The concept is analogous to that of using bend migration rates for estimation of long-term bedload transport rates in meandering rivers (see Ashmore and Church, 1998).

In some previous work, planform change has been used as part of interpretation of morphological change from cross-sections or DEM data (Goff and Ashmore 1994; Bertoldi et al., 2010; Williams et al., 2014). Recent research has focussed mainly on defining detailed bed morphology and morphological bedload budgeting related to technical developments for field measurement from 'hyper resolution' DEMS for bedload budgeting and as a basis for numerical model assessment (Wheaton et al., 2013;

Williams et al., 2014; Vericat et al, 2017). Combining these kinds of studies with planimetric measurements may yield valuable insights and reliable predictions of the morphodynamics of gravel braided rivers. This requires more extensive data sets and generalisation of empirical relationships, but planimetric change monitoring, possibly combined with predictions of reach-scale active layer depth (McLean and Church, 1999; Ashmore et al., 2018) presents one possible practical approach for surrogate bedload monitoring measurements. The empirical correlation between planimetric change and bedload has a physical basis because the planimetric change and total mobilized mass of bed material are correlated through coincident areas of change and related active layer depth (Ashmore et al., 2018, Peirce et al., 2018). Mobilized mass (volume), combined with path length, is a formal definition of bedload flux (see e.g. McLean and Church, 1999; Church, 2006).

If planimetric change is adequate for bedload prediction then topographic cross-section or DEM-based morphological surveys may not be needed for monitoring bedload transport (although obviously important for other reasons), and much larger data sets could be collected more rapidly because of the relative ease of planimetric mapping, especially with new aerial platforms provided by UAVs (Westoby et al., 2012; Woodget et al., 2014; Tamminga et al., 2015; Kelleher et al., 2018). Alternatively, planimetric data could be a useful source of data for filling time or spatial gaps in full morphological surveys. In any of these cases there is still a need to investigate the ‘throughput’ component of bedload during planform change events (Ashmore and Church, 1998) but there are indications that path length of transport may be of the order of the length scale of major braid bars which then sets the minimum length for monitoring without significant throughput. In addition, the data from the physical model experiments indicate that there is no missing ‘background’ gravel bedload flux occurring below the planimetric change threshold.

The planimetric change data are based on manual measurement (as is the case with similar data in Bertoldi et al., 2010). If larger areas and longer time periods are to be monitored, a more automated approach to change detection would be valuable. While separation of water and exposed gravel is easily accomplished by image analysis on a single image, the daily and hourly variation in lighting, reflection and water colour complicate the parameter selection. Apart from these image selection issues, the primary difficulty in automated analysis is reliably separating apparent changes due to water redistribution or slight local water level differences (which can occur on successive days even for the same discharge) from genuine changes in planform and bed morphology. In general, this is likely to cause systematic over-estimation relative to real change measured from careful visual assessment (Middleton, 2017). A general solution to this problem would enable much larger data sets to be collected and analyzed and so expand the empirical basis for these relationships of planform dynamics and bedload in braided rivers.

While the proglacial setting allows for a large number of daily measurements to be made in a short time period, the relatively small range of discharge in this setting means that the applicability to other types of flow regime remains to be assessed. Much larger magnitude, and longer duration events may change the morphodynamic regime and bar dynamics during large floods, for example in the case of the Waimakariri or Tagliamento (Hicks et al., 2002; Bertoldi et al., 2010), so changing the planform dynamics-bedload relationship. Sustained high discharge may also hamper planimetric measurements and cause more extensive and variable morphological changes during a single event. The planform-bedload relationship may potentially also be modified by the current condition of the river system more broadly, whether it is aggrading or degrading, but this is not known. Further observations across a range of settings and braided river types are needed to understand these possible differences in morphodynamics related to hydrological regime, river scale, river conditions, bed material mobility and morphodynamic regime.

Significant morphological changes are limited to 10-15 days during the four month meltwater season in the proglacial flow regime and occur in two or three small groups of successive days separated by periods of inactivity. This observation can be linked to classical discussions of magnitude and frequency of channel-forming events and effective discharge for bedload transport in rivers (Schmidt and Potyondy, 2004). Discharges greater than 11 $m^3 s^{-1}$ that produced planform change occur less than 20% of the time based on all seasonal flows on record and therefore less than 10% of the year. More investigation of the types of braiding processes occurring at different peak or event discharge is needed to develop a descriptive and quantitative magnitude-frequency analysis of braiding morphodynamics, in different hydrological regimes. Extended time lapse monitoring has obvious potential as a method for building observational data sets for doing this.

Grain size data for the bedload in the physical model also indicate events of a particular magnitude and rates of planimetric change may be associated with different gravel bed material mobility conditions. All discharges high enough to cause planimetric change showed selective mobility (all sizes are mobile but not in the same proportion as the bed material grain size distribution) and events with extensive planimetric and morphological change had bedload close to equal mobility (bed load size distribution very similar to that of the bed material) including having D_{90} of the bed load very similar to that of the bulk bed material (Mueller and Pitlick, 2014). This is similar to results from other experiments in the same braided river model as was used here (Peirce et al., 2018) and is consistent with the recent suggestion of Mackenzie et al. (2017) that there is a close and sensitive association of bed material particle size distribution and mobility with braiding morphodynamics. If further experimentation proves this relationship to be reliable, then the relative magnitude of the planimetric change may be used to infer information on bedload grain size distribution and bed material mobility as well as bedload transport rate.

Conclusion

The prediction of both planform change processes and bedload transport are key issues in fluvial geomorphology and the study of braided rivers specifically (Davies, 1987; Gomez, 1991; Church, 2006; Luchi et al., 2007). Analysis of an extensive set of time-lapse images over two years of planform change in a proglacial braided gravel-bed river showed that areas of planform change have a continuous positive relationship with daily meltwater hydrograph peak discharge and total flow volume, and a clear threshold discharge below which no detectable planform change occurred. Significant planimetric change was limited to 10-15 days each meltwater season of about four months. Topographic measurements collected from previous studies at the same site showed a similar threshold for change and a similar variability in rates of change at different discharges. Complementary physical model experiments for the field site confirmed this relationship and also demonstrated a correlation between planimetric change, volume and area of morphological change from photogrammetric DEMs of the model, and event bedload transport. Bedload transport and morphological change had threshold discharges very similar to the planimetric change data. Very little bedload transport of the gravel size fraction occurred without measurable planimetric change. The major types of braiding planform processes (avulsion, major channel migration, braid bar formation/erosion etc.) were associated with larger magnitude discharge and planimetric changes and higher bedload transport rates, while smaller events accomplished local bank and bed erosion/deposition and bar accretion. Bed material particle mobility increased with increasing rates of bedload transport, planimetric, and morphological change, approaching equal mobility at the highest rates of morphological change.

The physical model results also show the close relationship between the rates of planimetric change, morphological change (erosion-deposition volumes) and rates of bedload transport in a proglacial system. Consequently, it may be possible to use continuous monitoring of planimetric change as a method for understanding planform dynamics of braiding, while also producing an associated record of bedload transport rate and its temporal and spatial variability. This would allow these changes to be continuously monitored more easily, cost-effectively, extensively and continuously in time and so would complement analysis of detailed morphological change from hyper-scale topography, provide important data for helping to develop improved understanding and prediction of several important aspects of braided river morphodynamics, and support validation of numerical modeling of braiding morphodynamics and bedload.

With further observational data and generalization to other rivers, planimetric change monitoring can be an important source of data for investigating braiding river morphodynamics, and has the potential to be a valuable surrogate for bedload transport measurement in gravel-bed braided rivers and perhaps in other laterally-active river types.

Acknowledgements

This research was supported by a Natural Sciences and Engineering Research Council Discovery Grant (41186-2012) to Peter Ashmore. Flume construction was supported by the Canada Foundation for Innovation and Newalta Resources Inc. Thank you to everyone who assisted with field and lab work including Matilde Welber, Sarah Peirce, Elizabeth Sutherland and Danielle Barr.

References:

Arscott DB, Tockner K, van der Nat D, Ward JV. 2002. Aquatic Habitat Dynamics along a Braided Alpine River Ecosystem (Tagliamento River, Northeast Italy). *Ecosystems*, ***5***, 802–814. https://doi.org/10.1007/s10021-002-0192-7.

Ashmore PE. 1982. Laboratory modelling of gravel braided stream morphology. *Earth Surface Processes and Landforms*, ***7***, 201–225. https://doi.org/10.1002/esp.3290070301

Ashmore P. 1988. Bed load transport in braided gravel-bed stream models. *Earth Surface Processes and Landforms*, ***13***, 677–695.

Ashmore P. 1991. Channel morphology and bed load pulses in braided, gravel-bed streams. *Geografiska Annaler*, ***73***, 37-52.

Ashmore P. 2013. Morphology and Dynamics of Braided Rivers. In Treatise on Geomorphology, Shroder J and Wohl E (eds). Academic Press: San Diego; CA, vol. 9, Fluvial Geomorphology, pp. 289–312. https://doi.org/10.1016/B978-0-12-374739-6.00242-6

Ashmore P, Bertoldi W, Tobias Gardner J. 2011. Active width of gravel-bed braided rivers. *Earth Surface Processes and Landforms*, ***36***, 1510–1521. https://doi.org/10.1002/esp.2182.

Ashmore P, Church M. 1998. Sediment transport and river morphology: a paradigm for study. In Gravel-Bed Rivers in the Environment: 115–148.

Ashmore P, Parker G. 1983. Confluence Scour in Coarse Braided Streams. *Water Resources Research*, ***19***(2), 392–402.

Ashmore P, Sauks E. 2006. Prediction of discharge from water surface width in a braided river with implications for at-a-station hydraulic geometry. *Water Resources Research*, ***42***, 1–11. https://doi.org/10.1029/2005WR003993.

Ashmore P, Peirce S, Leduc P. 2018. Expanding the "active layer": Discussion of Church and Haschenburger (2017) What is the "active layer"? *Water Resources Research*, ***53***, 5–10. https://doi.org/10.1002/2017WR022438

Bertoldi W, Ashmore P, Tubino M. 2009. A method for estimating the mean bed load flux in braided rivers. *Geomorphology*, ***103***, 330–340. https://doi.org/10.1016/j.geomorph.2008.06.014

Bertoldi W, Gurnell A, Surian N, Tockner K, Zanoni L, Ziliani L, Zolezzi G. 2009. Understanding reference processes: linkages between river flows, sediment dynamics and vegetated landforms along the Tagliamento River, Italy. *River Research and Applications*, ***25***, 501–516. https://doi.org/10.1002/rra.1233

Bertoldi W, Zanoni L, Tubino M. 2010. Assessment of morphological changes induced by flow and flood pulses in a gravel bed braided river: The Tagliamento River (Italy). *Geomorphology*, ***114***(3), 348–360. https://doi.org/10.1016/j.geomorph.2009.07.017

Brasington J, Rumsby BT, Mcvey RA. 2000. Monitoring and modelling morphological change in a braided gravel-bed river using high resolution GPS-based survey. *Earth Surface Processes and Landforms* ***25***, 973–990.

Bridge JS. 1993. The interaction between channel geometry, water flow, sediment transport and deposition in braided rivers. In J. L. Best and C. S. Bristow (Eds.), Braided Rivers: 13–71.

Chandler J, Ashmore P, Paola C, Gooch M, Varkaris F. 2002. Monitoring river-channel change using terrestrial oblique digital imagery and automated digital photogrammetry. *Annals of the Association of American Geographers*, ***92***(4), 631–644. https://doi.org/10.1111/1467-8306.00308

Chew LC, Ashmore PE. 2001. Channel adjustment and a test of rational regime theory in a proglacial braided stream. *Geomorphology*, ***37***, 43–63.

Church M. 2006. Bed Material Transport and the Morphology of Alluvial River Channels. *Annual Review of Earth and Planetary Sciences*, ***34***(1), 325–354. https://doi.org/10.1146/annurev.earth.33.092203.122721

Church M, Ferguson RI. 2015. Morphodynamics: Rivers beyond steady state. *Water Resources Research*, ***51***, 1883–1897. https://doi.org/10.1002/2014WR016862.

Davies TRH. 1987. Problems of Bed Load Transport in Braided Gravel-bed Rivers. In Sediment Transport in Gravel-Bed Rivers, Thorne, C.R., Bathurst, J.C., and Hey, R.D.(eds). John Wiley and Sons Ltd.

East AE, Jenkins KJ, Happe PJ, Bountry JA, Beechie TJ, Mastin MC, Sankey JB, Randle TJ. 2017. Channel-planform evolution in four rivers of Olympic National Park, Washington, USA: the roles of physical drivers and trophic cascades. *Earth Surface Processes and Landforms*, ***42***, 1011–1032. https://doi.org/10.1002/esp.4048.

Gaeuman, D. A., Schmidt, J. C., & Wilcock, P. R. (2003). Evaluation of in-channel gravel storage with morphology-based gravel budgets developed from planimetric data. *Journal of Geophysical Research*, *108*(F1), 1-16. https://doi.org/10.1029/2002JF000002

Garcia Lugo GA, Bertoldi W, Henshaw AJ, Gurnell AM. 2015. The effect of lateral confinement on gravel bed river morphology. *Water Resources Research*, ***51***, 7145–7158. https://doi.org/10.1002/2015WR017081

Goff J, Ashmore P. 1994. Gravel transport and morphological change in braided Sunwapta River, Alberta, Canada. *Earth Surface Processes and Landforms* **19**: 195–212.

Gomez B. 1991. Bedload transport. *Earth Sciences Reviews* **31**: 89–132.

Ham, DG, Church, M. (2000). Bed-material transport estimated from channel morphodynamics: Chilliwack River, British Columbia. *Earth Surface Processes and Landforms*, ***25***, 1123–1142.

Haschenburger JK. 2013. Tracing river gravels: Insights into dispersion from a long-term field experiment. *Geomorphology*, ***200***, 121–131. https://doi.org/10.1016/j.geomorph.2013.03.033

Hicks DM, Duncan MJ, Walsh JM, Westaway RM, Lane SN. 2002. New views of the morphodynamics of large braided rivers from high-resolution topographic surveys and time-lapse video. *The Structure, Function and Management Implications of Fluvial Sedimentary Systems* **276,** 373–380.

Hoey TB, Sutherland AJ. 1991. Channel morphology and bedload pulses in braided rivers: a laboratory study. *Earth Surface Processes and Landforms*, ***16***, 447–462.

Hundey EJ, Ashmore PE. 2009. Length scale of braided river morphology. *Water Resources Research*, ***45***, 1–9. https://doi.org/10.1029/2008WR007521.

Javernick L, Brasington J, Caruso B. 2014. Modeling the topography of shallow braided rivers using Structure-from-Motion photogrammetry. *Geomorphology*, ***213***, 166–182. https://doi.org/10.1016/j.geomorph.2014.01.006

Javernick L, Hicks DM. Measures R, Caruso B, Brasington J. 2016. Numerical modelling of braided rivers with Structure-from-Motion derived terrain models. *River Research and Applications*, ***32***, 1071–1081. https://doi.org/10.1002/rra

Kasprak A, Wheaton JM, Ashmore PE, Hensleigh JW, Peirce, S. 2015. The relationship between particle travel distance and channel morphology : Results from physical models of braided rivers. *Journal of Geophysical Research: Earth Surface*, ***120***, 55–74. https://doi.org/10.1002/2014JF003310.

Kelleher C, Scholz C, Condon L, Reardon M. 2018. Drones in geoscience research: The sky is the only limit. *EOS* ***99****.* https://doi.org/10.1029/2018EO092269.

Lane SN, Westaway RM, Hicks DM. 2003. Estimation of erosion and deposition volumes in a large, gravel-bed, braided river using synoptic remote sensing. *Earth Surface Processes and Landforms*, ***28***, 249–271. https://doi.org/10.1002/esp.483

Leduc P, Ashmore P, Sjogren D. 2017. Technical note: Stage and water width measurement of a mountain stream using a simple time-lapse camera. *Hydrology and Earth System Sciences,* 1–17. https://doi.org/10.5194/hess-2017-285.

Lenzi MA, Mao L, Comiti F. 2004. Magnitude-frequency analysis of bed load data in an Alpine boulder bed stream. *Water Resources Research* ***40***, 1–12. https://doi.org/10.1029/2003WR002961

Liu Y, Métivier F, Lajeunesse É, Lancien P, Narteau C, Ye B, Meunier P. 2008. Measuring bedload in gravel-bed mountain rivers: averaging methods and sampling strategies. *Geodinamica Acta*, **2**, 81–92. https://doi.org/10.3166/ga.21.81-92

Luchi R, Bertoldi W, Zolezzi G, Tubino M. 2007. Monitoring and predicting channel change in a free-evolving, small Alpine river: Ridanna Creek (North East Italy). *Earth Surface Processes and Landforms* ***32***: 2104–2119. https://doi.org/10.1002/esp.1511

Mackenzie LG, Eaton BC. 2017. Large grains matter: contrasting bed stability and morphodynamics during two nearly identical experiments. *Earth Surface Processes and Landforms* ***42***, 1287–1295. https://doi.org/10.1002/esp.4122

Mao L, Picco L, Lenzi MA, Surian N. 2017. Bed material transport estimate in large gravel-bed rivers using the virtual velocity approach. *Earth Surface Processes and Landforms* ***42***, 595–611. https://doi.org/10.1002/esp.4000

Mao L, Surian N. 2010. Observations on sediment mobility in a large gravel-bed river. *Geomorphology* ***114***, 326–337. https://doi.org/10.1016/j.geomorph.2009.07.015

McKenna Neuman C, Ashmore P, Bennett S J. 2013. Laboratory and Experimental Geomorphology: Examples from Fluvial and Aeolian Systems. In Treatise on Geomorphology, Shroder J and Wohl E (eds). Academic Press: San Diego; CA, vol. 1, The Foundation of Geomorphology, pp. 289–312, 325–348. https://doi.org/10.1016/B978-0-12-374739-6.00017-8

McLean DG, Church M. 1999. Sediment transport along lower Fraser River 2. Estimates based on the long-term gravel budget. *Water Resources Research* ***35***, 2549–2559.

Meunier P, Métivier F, Lajeunesse E, Mériaux AS, Faure J. 2006. Flow pattern and sediment transport in a braided river: The “torrent de St Pierre” (French Alps). *Journal of Hydrology* ***330,*** 496–505. https://doi.org/10.1016/j.jhydrol.2006.04.009.

Middleton, L. (2017). The relationship of planform change and bedload transport in a proglacial gravel-bed braided river. MSc Thesis. Department of Geography, University of Western Ontario.

Morgan JA, Brogan DJ, Nelson PA. 2016. Application of Structure-from-Motion photogrammetry in laboratory flumes. *Geomorphology* ***276***, 125–143. https://doi.org/10.1016/j.geomorph.2016.10.021

Mosley MP. 1982. Analysis of the Effect of Changing Discharge on Channel Morphology and Instream Uses in a Braided River, Ohau River, New Zealand. *Water Resources Research* ***18***, 800–812. https://doi.org/10.1029/WR018i004p00800

Mueller ER, Pitlick J. 2014. Sediment supply and channel morphology in mountain river systems: 2. Single thread to braided transitions. *Journal of Geophysical Research: Earth Surface* ***119***, 1–26. https://doi.org/10.1002/2013JF003045.

Papangelakis E, Hassan MA. 2016. The role of channel morphology on the mobility and dispersion of bed sediment in a small gravel-bed stream. *Earth Surface Processes and Landforms* ***41***, 2191–2206. https://doi.org/10.1002/esp.3980

Peakall J, Ashworth P, Best JL. 1996. Physical Modelling in Fluvial Geomorphology: Principles, Applications and Unresolved Issues. In *The Scientific Nature of*

Geomorphology: Proceedings from the 17^{th} *Binghamton Symposium in Geomorphology, 27-29 September, 1996,* 221-253.

Peirce S, Ashmore P, Leduc P. 2018. The variability in the morphological active width: Results from physical models of gravel-bed braided rivers. *Earth Surface Processes and Landforms*. https://doi.org/10.1002/esp.4400

Picco L, Mao L, Cavalli M, Buzzi E, Rainato R, Lenzi MA. 2013. Evaluating short-term morphological changes in a gravel-bed braided river using terrestrial laser scanner. *Geomorphology* ***201***: 323–334. https://doi.org/10.1016/j.geomorph.2013.07.007

Pyrce RS, Ashmore PE. 2005. Bedload path length and point bar development in gravel-bed river models. *Sedimentology* ***52***, 839–857. https://doi.org/10.1111/j.1365-3091.2005.00714.x

Recking A, Piton G, Vazquez-Tarrio D, Parker G. 2016. Quantifying the Morphological Print of Bedload Transport. *Earth Surface Processes and Landforms,* ***41***: 809–822. https://doi.org/10.1002/esp.3869

Redolfi M, Bertoldi W, Tubino M, Welber M. 2018. Bed Load Variability and Morphology of Gravel Bed Rivers Subject to Unsteady Flow: A Laboratory Investigation. *Water Resources Research,* 1–21. https://doi.org/10.1002/2017WR021143

Schmidt LJ, Potyondy JP. 2004. Quantifying Channel Maintenance Instream Flows: An Approach for Gravel-Bed Streams in the Western United States. Gen. Tech. Rep. RMRS-GTR-128. Fort Collins, CO: U.S. Department of Agriculture, Forest Service, Rocky Mountain Research Station.

Schneider, C. A., Rasband, W. S., & Eliceiri, K. W. 2012. NIH Image to ImageJ: 25 years of Image Analysis. *Nature Methods*, ***9***(7), 671–675. https://doi.org/10.1038/nmeth.2089

Schvidchenko AB, Kopaliani ZD. 1998. Hydraulic Modeling of Bed Load Transport in Gravel-Bed Laba River. *Journal of Hydraulic Engineering* ***124***, 778–785.

Tamminga AD, Eaton BC, Hugenholtz CH. 2015. UAS-based remote sensing of fluvial change following an extreme flood event. *Earth Surface Processes and Landforms* ***40****,* 1464–1476. https://doi.org/10.1002/esp.3728

Vericat D, Wheaton JM, Brasington J. 2017. Revisiting the Morphological Approach: Opportunities and Challenges with Repeat High-Resolution Topography. In *Gravel-Bed Rivers: Processes and Disasters*. John Wiley and Sons, Ltd: 121–158. https://doi.org/10.1002/9781118971437.ch5

Warburton, J. (1996). Active braidplain width, bedload transport and channel morphology in a model braided river. *Journal of Hydrology* ***(NZ), 35***(2), 259–285.

Warburton J, Davies TRH, Mandl MG. 1993. A meso-scale field investigation of channel change and floodplain characteristics in an upland braided gravel-bed river, New Zealand. In Nest, J L and Bristow, C S (eds), 1993, *Braided Rivers,* Geological Society Special Publication No. **75,** 241-255.

Westoby MJ, Brasington J, Glasser NF, Hambrey MJ, Reynolds JM. 2012. “Structure-from-Motion” photogrammetry: A low-cost, effective tool for geoscience applications*. Geomorphology **179***, 300–314. https://doi.org/10.1016/j.geomorph.2012.08.021

Wheaton JM, Brasington J, Darby SE, Kasprak A, Sear D, Vericat D. 2013. Morphodynamic signatures of braiding mechanisms as expressed through change in sediment storage in a gravel-bed river. *Journal of Geophysical Research: Earth Surface **118***, 759–779. https://doi.org/10.1002/jgrf.20060

Williams, R. D. 2012. DEMs of Difference. *Geomorphological Techniques*, 1–17.

Williams RD, Brasington J, Hicks M, Measures R, Rennie CD, Vericat D. 2013. Hydraulic validation of two-dimensional simulations of braided river flow with spatially continuous aDcp data. *Water Resources Research, **49***, 5183–5205. https://doi.org/10.1002/wrcr.20391

Williams RD, Brasington J, Vericat D, Hicks DM. 2014. Hyperscale terrain modelling of braided rivers: fusing mobile terrestrial laser scanning and optical bathymetric mapping. *Earth Surface Processes and Landforms **39***: 167–183. https://doi.org/10.1002/esp.3437

Williams R, Brasington J, Vericat D, Hicks DM., Labrosse F, Neal M. 2011. Monitoring Braided River Change Using Terrestrial Laser Scanning and Optical Bathymetric Mapping. *Developments in Earth Surface Processes **15***. 507-532. https://doi.org/10.1016/B978-0-444-53446-0.00020-3

Williams RD, Measures R, Hicks DM, Brasington J. 2016. Assessment of a numerical model to reproduce event-scale erosion and deposition distributions in a braided river. *Water Resources Research **52**:* 6621–6642. https://doi.org/10.1002/2015WR018491

Williams RD, Rennie CD, Brasington J, Hicks DM, Vericat D. 2015. Linking the spatial distribution of bedload transport to morphological change during high-flow events in a shallow braided river. *Journal of Geophysical Research: Earth Surface **120***: 604–622. https://doi.org/10.1002/2014JF003346

Woodget AS, Carbonneau PE, Visser F, Maddock IP. 2015. Quantifying submerged fluvial topography using hyperspatial resolution UAS imagery and structure from motion photogrammetry. *Earth Surface Processes and Landforms **40***, 47–64. https://doi.org/10.1002/esp.3613

Young WJ, Davies TRH. 1991. Bedload transport processes in a braided gravel-bed river model. *Earth Surface Processes and Landforms* ***16***, 499-511. https://doi.org/10.1002/esp.3290160603

Young WJ, Warburton J. 1996. Principles and practice of hydraulic modelling of braided gravel-bed rivers. *Journal of Hydrology (NZ)* ***35***: 175–198. https://doi.org/10.1016/S0301-9322(97)80098-53

Ziliani L, Surian N, Coulthard TJ, Tarantola S. 2013. Reduced-complexity modeling of braided rivers: Assessing model performance by sensitivity analysis, calibration, and validation. *Journal of Geophysical Research: Earth Surface* ***118***, 2243–2262. https://doi.org/10.1002/jgrf.20154

Table 1*:* The Pearson's Correlation computed between the area of planform change in relation to both volumes of morphological change and total bedload transport mass. PCC= Pearson's Correlation Coefficient, n= number of observations.

	Morphological Change	**Total Bedload Transport**
PCC	0.928	0.586
Significance (p-value)	<0.0001	0.004
n	12	12

Supporting Information

Rates of planimetric change in a proglacial gravel-bed braided river: field measurement and physical modeling

L. Middleton*[1], P. Ashmore[1], P. Leduc[1], D. Sjogren[2]

[1] Department of Geography, University of Western Ontario, London, Ontario, Canada, N6A5C2

*Corresponding author: lmiddle7@uwo.ca

[2] Department of Geography, University of Calgary, Calgary, Alberta, Canada

The supporting information consists of two videos of diurnal hydrographs in the field and scaled down in the laboratory setting.

The field video (Sunwapta_Video_2012) shows a high flow period during the 2012 study period from July 7-22. The flow direction is from left to right and spans a distance of 100m at the bottom of the camera frame. The time and date of each image can be seen in the top right-hand corner with an image taken every half hour from 0600 to 2000 everyday. The first two diurnal hydrographs from July 7-9 (0:00:00-0:00:10) can be seen to produce either no, or minor, planimetric changes. As discharge increases on July 9th, large planimetric changes can be observed through the erosion of, and development of new braid bars and lateral migration of the primary channels. Large scale planimetric change can be observed until the morning of July 14th (0:00:10-0:00:30) when rates of planimetric change decrease for a few days. The river planform changes significantly again from the 16th to the 21st of July (0:00:40-00:01:00).

The laboratory video (Flume_Hydrograph_Video) shows the entire sequence of hydrograph experiments run in the physical model, seen in Figure 12. The flow direction if from left to right and cover a longitudinal distance of approximately 10m. Images were taken each minute during experimental runs and document both the rising and falling limb of the hydrograph, not possible in the field due to the night-time loss of images on the falling stage. The two lowest peak discharges (hydrograph experiments 1, 4, 5, 8, 9, and 12) produce very minor, if any, planimetric changes. As the peak discharge increases to the second highest peak (hydrograph experiments 2, 6 and 10) we observe limited areas of planform change, including secluded areas of bank erosion and deposition around the primary channel. The highest peak (hydrograph experiments 3, 7 and 11) can be seen to produce large-scale planimetric changes as channels shift and laterally migrate, drastically altering the planform position.

a) 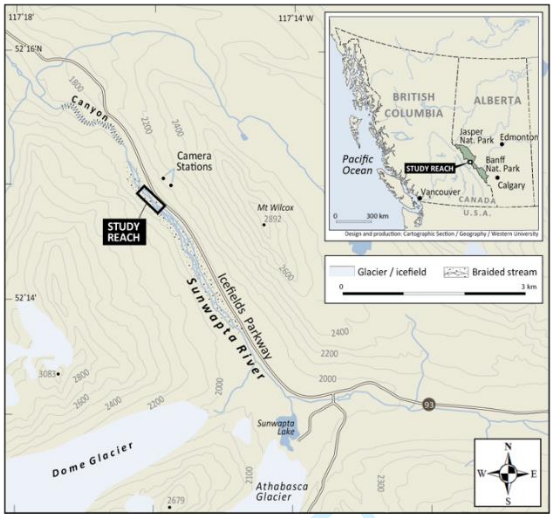

b) 

Figure 1 (a) The location of the study reach along the Icefields Parkway and in relation to the WSC gauge. The Sunwapta River begins at the outlet of Sunwapta Lake, flowing North-West. The camera locations identified in (a) can be seen in (b), flow direction is towards the camera.

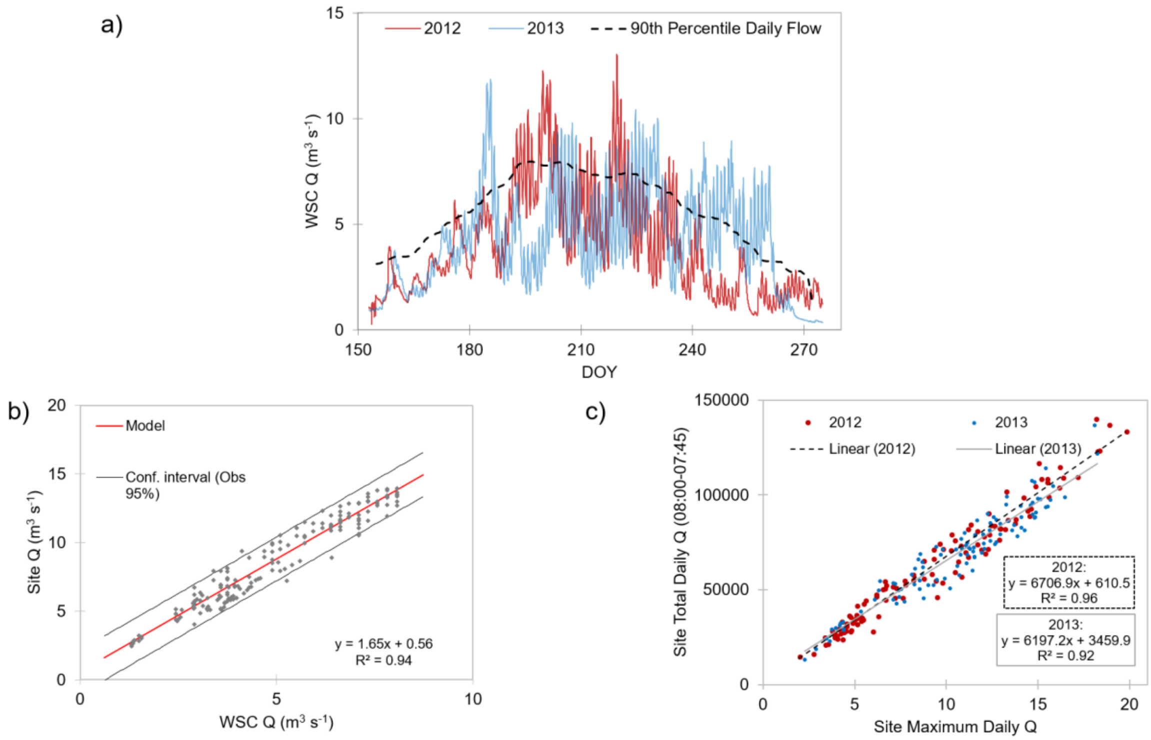

Figure 2 (a)15-minute discharge (Q) readings during the meltwater seasons of 2012 and 2013 (June 1-September 30, Day of the Year- DOY- 153-274) in relation to the daily historical 90th percentile flow. (b) The rating curve developed to determine the discharge at the site based on the WSC discharge with the linear regression plotted in red (model) and the 95% confidence interval shown. (c) The relationship between maximum daily discharge and total daily discharge over a diurnal hydrograph (08:00-07:45) and the linear regression line plotted for both 2012 and 2013.

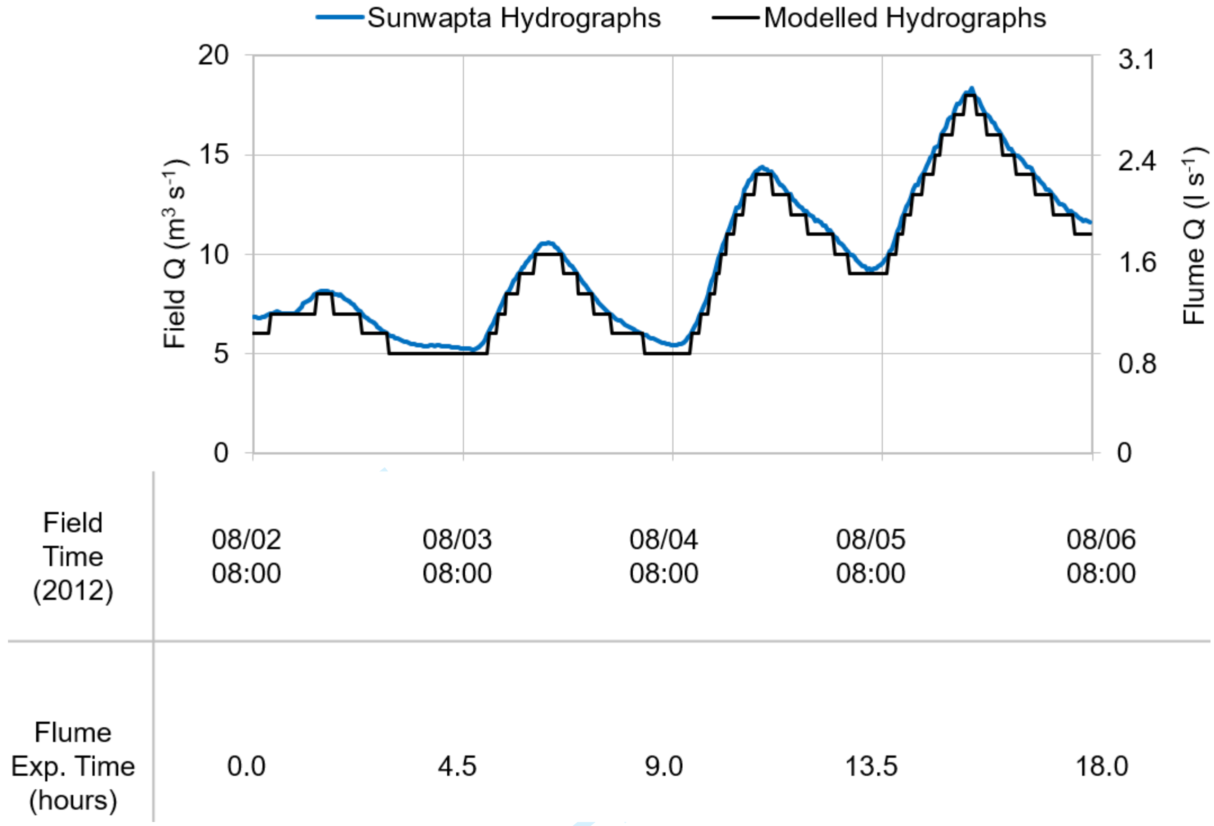

Figure 3 Selected representative hydrographs from the Sunwapta River in blue, showing the typical meltwater cycle from 8 am – 8 am. The replicated physical model hydrograph experiments are in black, with the equivalent discharge (Q) and time scaled down.

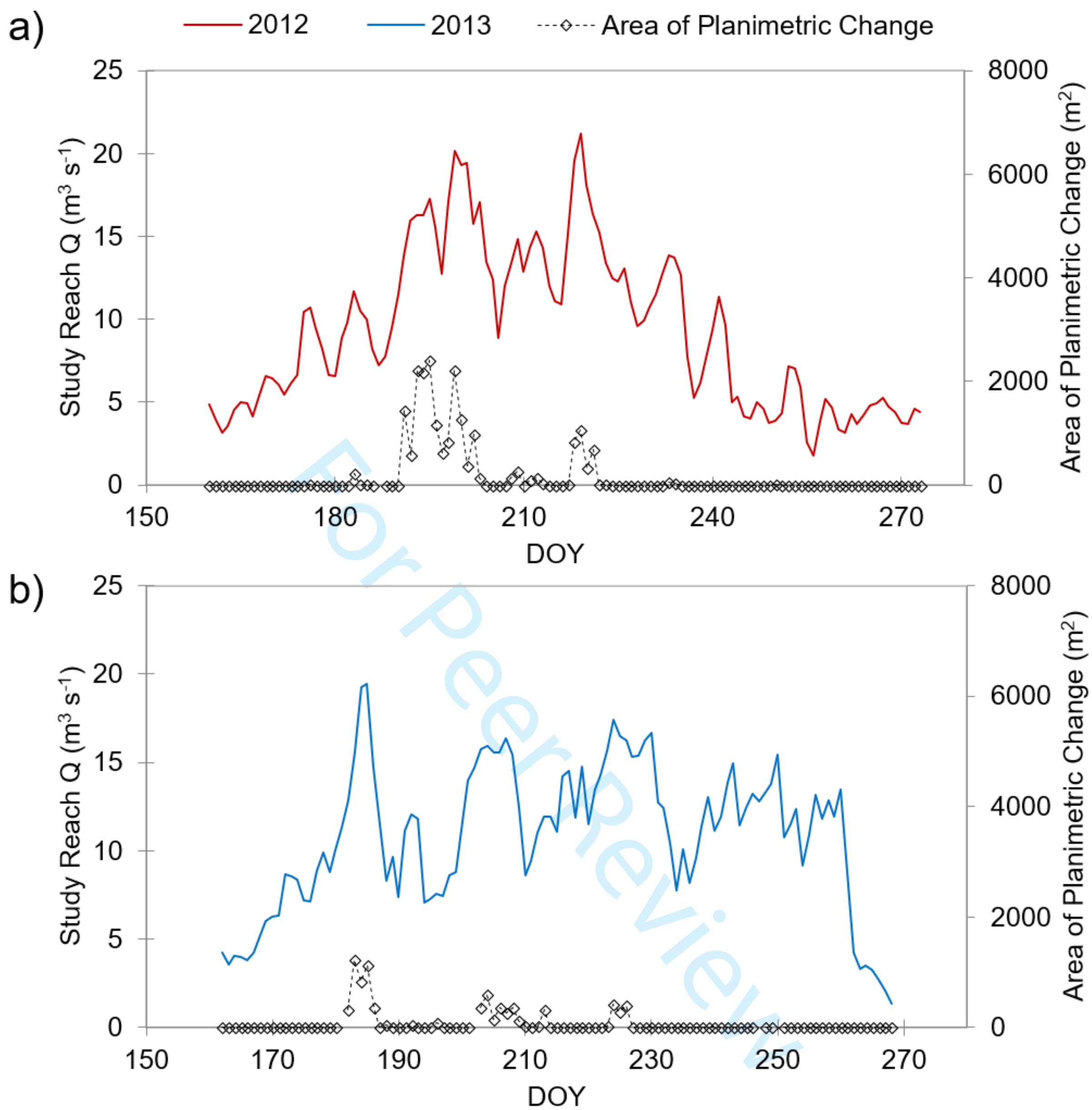

Figure 4 The (a) 2012 and (b) 2013 meltwater seasons studied from June-September (Day of the Year- DOY- 153-274) with the relationship between maximum daily discharge (Q) and area of planimetric change throughout the season.

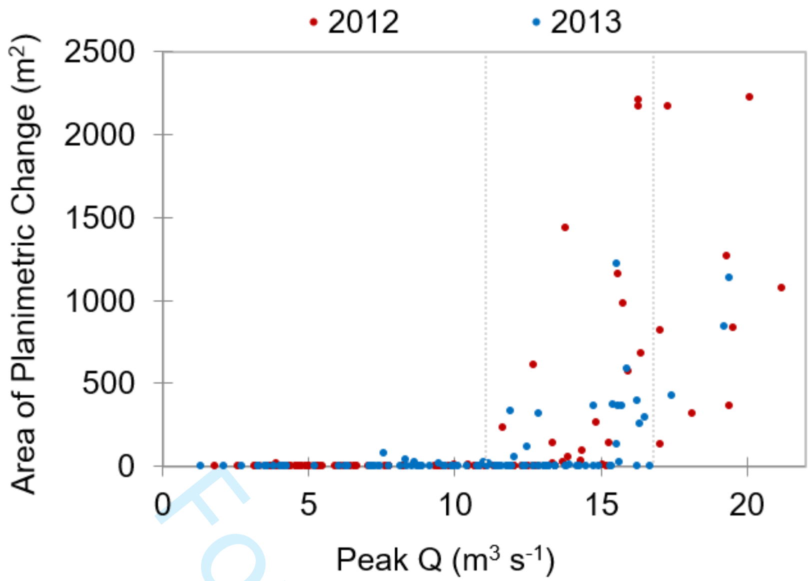

Figure 5 The relationship between measured areas of planimetric change over a daily hydrograph and daily peak discharge (Q) for the 2012 (red) and 2013 (blue) meltwater seasons. Vertical dashed lines indicate the two thresholds discussed.

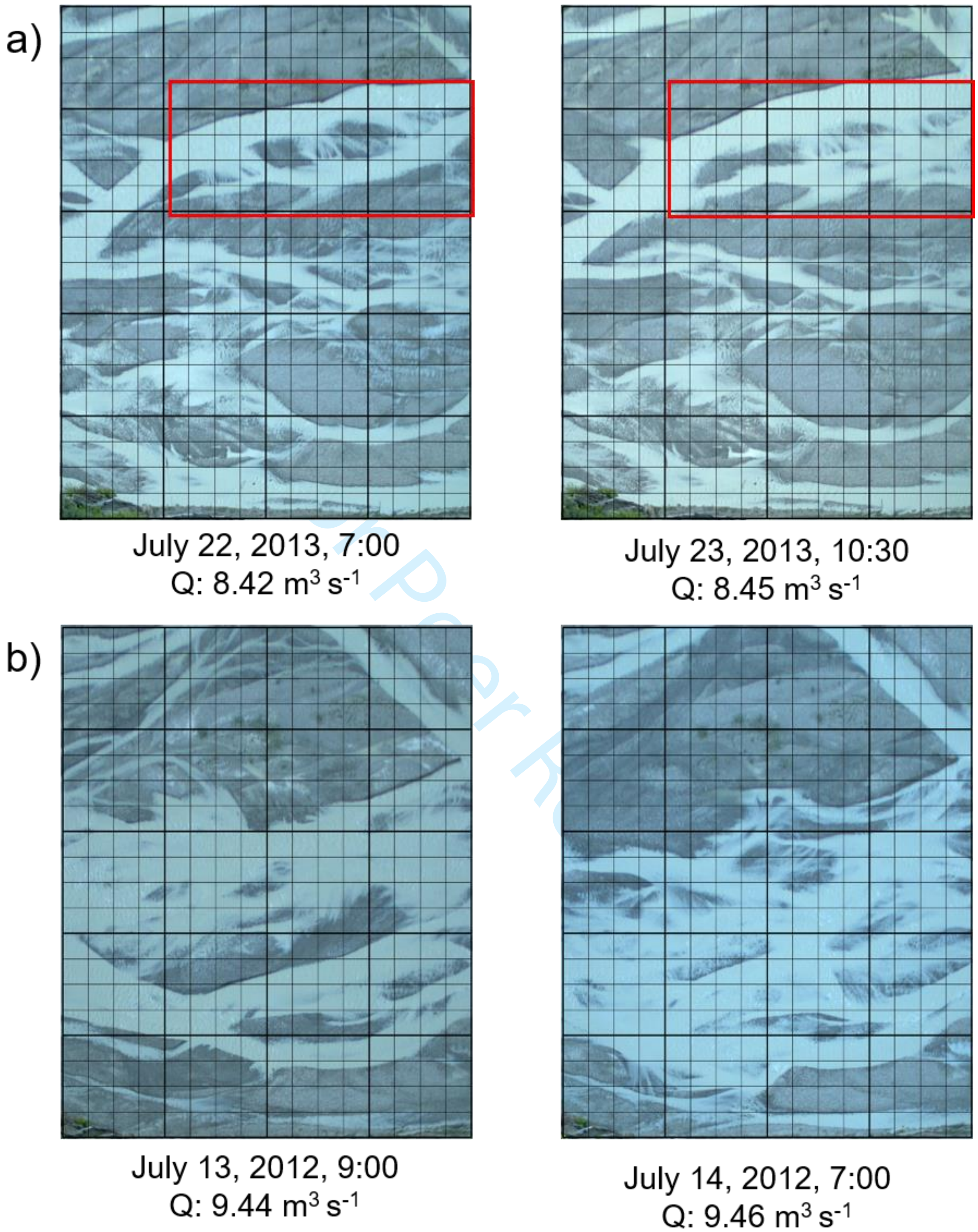

Figure 6 An example of planimetric changes measured seen in (a) smaller areas of bank erosion highlighted in red, peak daily discharge of 15.9 $m^3 s^{-1}$ and (b) large scale channel change, peak daily discharge of 17.3 $m^3 s^{-1}$. Flow direction is left to right and river width is ~ 120 m.

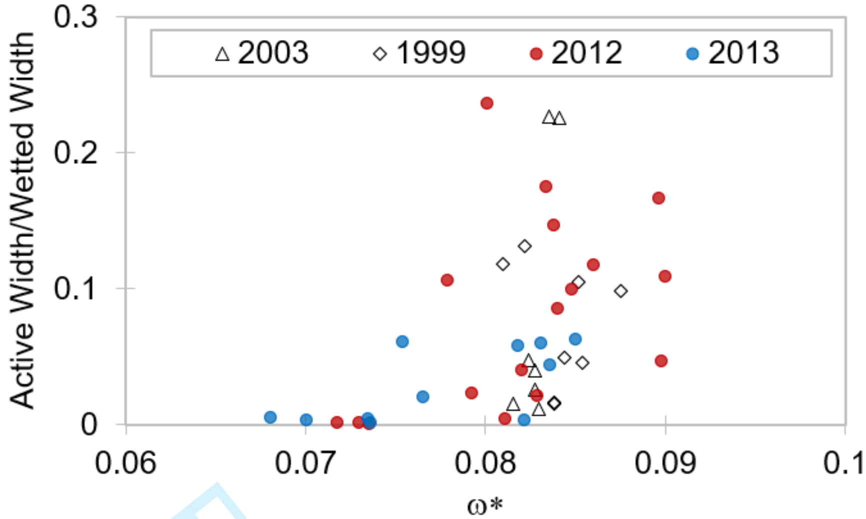

Figure 7 The relationship between previous morphological measurements made in the field in 1999 and 2003 and dimensionless stream power (ω*) compared to planimetric measurements completed for this study. Days with no morphological or planimetric change detected have not been plotted.

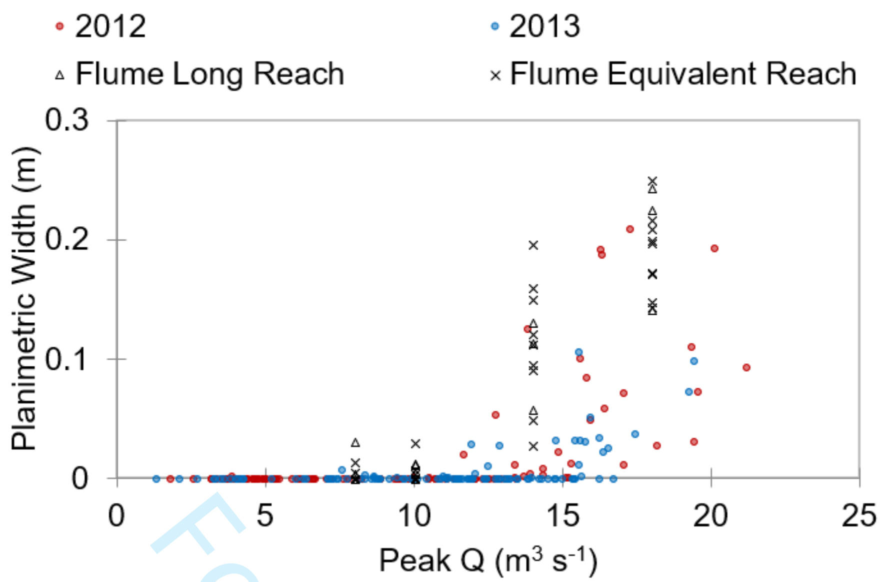

Figure 8 The relationship between the planimetric width and discharge (Q) in the field and equivalent measurements in the physical model based on both a longer, and an equivalent reach length to the field. Physical model peak hydrograph discharge has been scaled up to field equivalent.

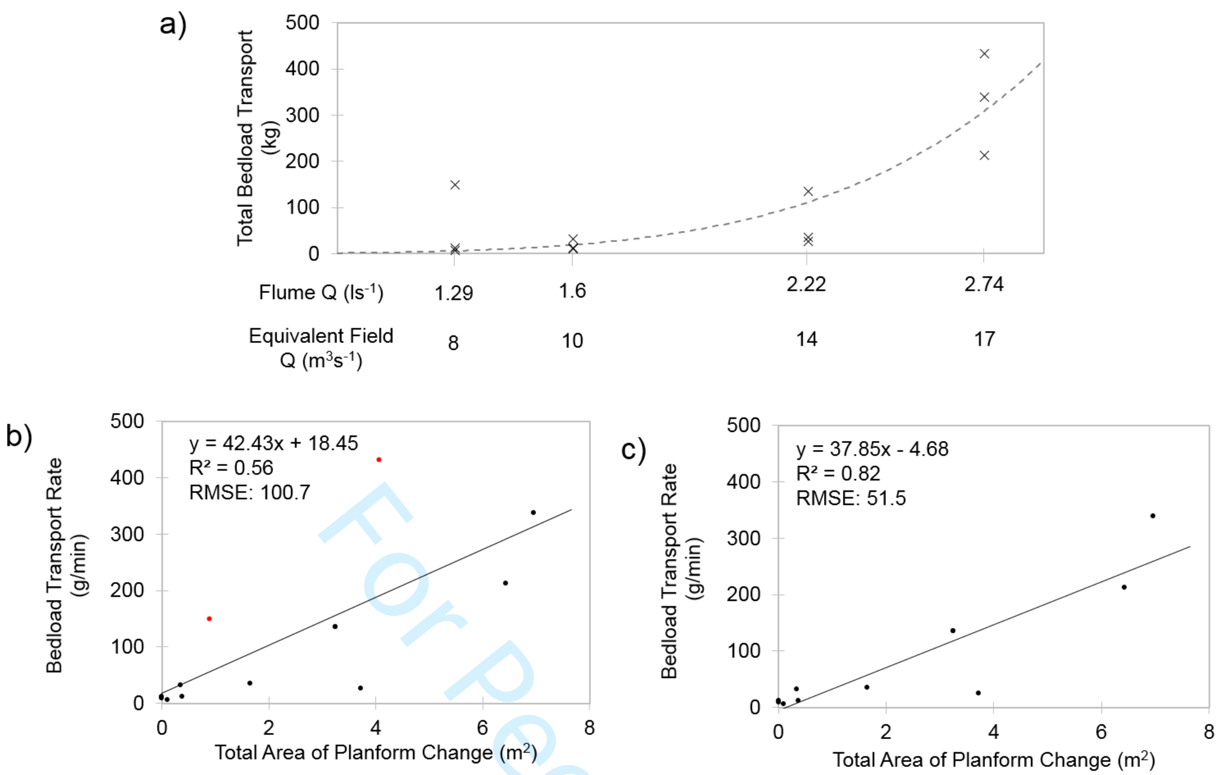

Figure 9 (a) The relationship between peak hydrograph discharge (Q) and total bedload transport. The grey, dashed line represents the power function through all observations. (b)The overall relationship between simultaneous measurements of bedload transport and areas of planimetric change over a hydrograph experiment with the analogous conditions of runs 11 and 12 in red. (c) The relationship between simultaneous bedload and areas of planimetric change plotted without experiments 11 and 12.The linear regression model and 95% confidence interval is plotted in both (b) and (c), highlighting the difference to the planform-bedload relation when the primary channel hits a hard boundary, reducing the ability to braid, compared to freely-mobile channels.

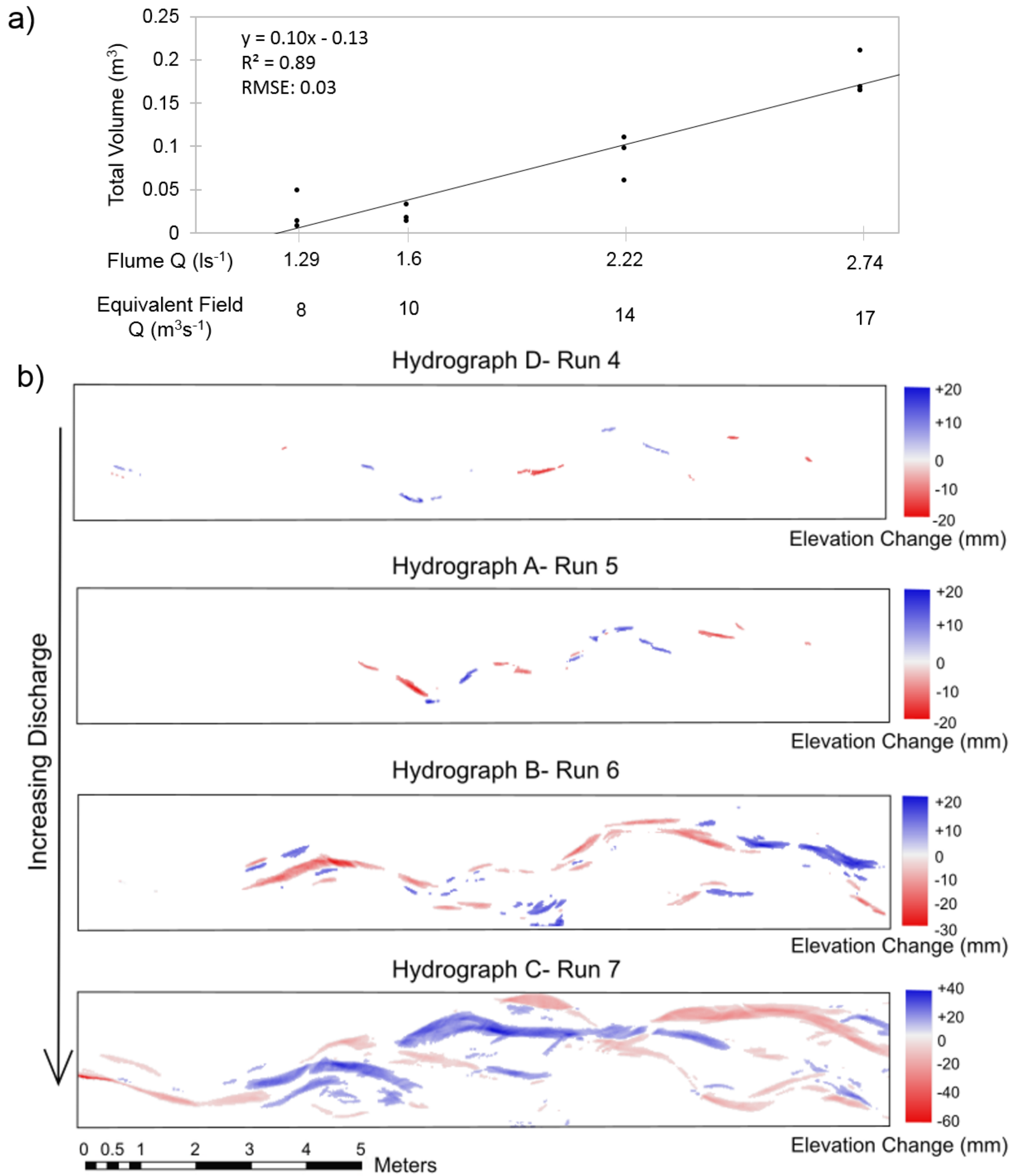

Figure 10 (a) Volumes of morphological change increased in relation to peak hydrograph discharge (Q). The linear regression model is plotted with the equation and 95% confident interval shown. (b) The area of change as well as the amplitude of topographic change (active layer thickness- Ashmore et al. 2018) increased, shown in a series of DEMs of Difference generated from four consecutive hydrograph experiments with increasing peak discharges. Flow is from left to right.

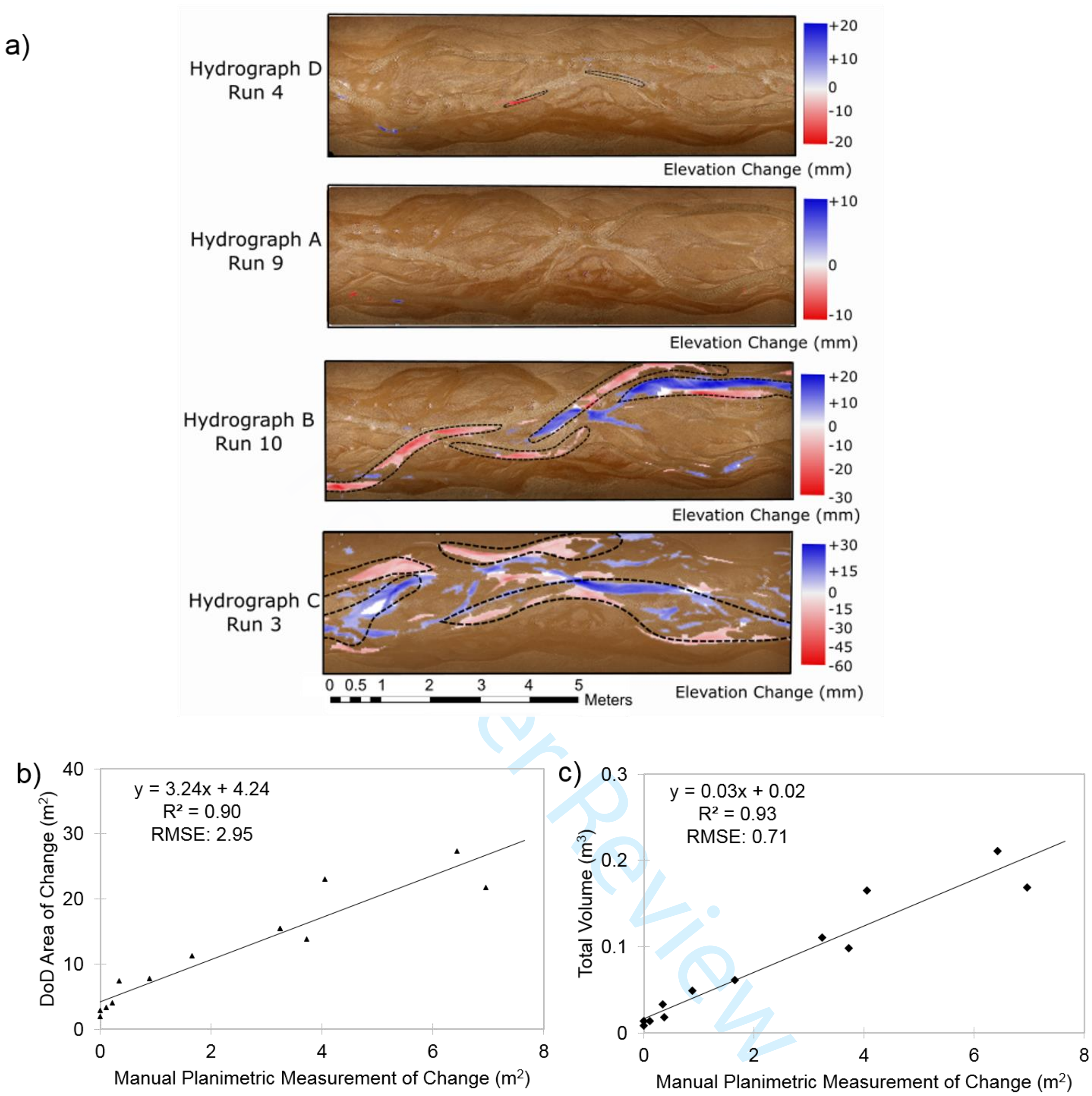

Figure 11 (a) A series of planimetric change maps with increasing discharge from top to bottom. Visual planimetric change is outlined in the black dotted line. Areas of morphological change from the DoDs are seen in blue (deposition) and red (erosion). Flow is from left to right. The relationship between simultaneous measurements of manual measured areas of planimetric chance and (b) the **area** over which morphological change was mapped on the DoD and (c) the **volume** of morphological change from the DoD. The linear regression model of both (b) and (c) is plotted with the equation and 95% confident interval.

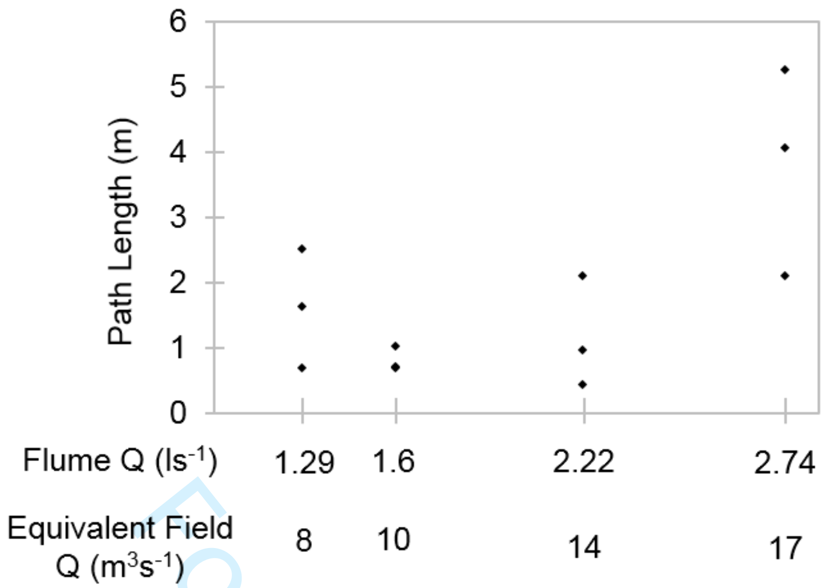

Figure 12 The relationship between particle path length and peak hydrograph discharge (Q).

a)

Hydrograph Experiment	A	B	C	D	A	B	C	D	A	B	C	D
Exp. Run #:	1	2	3	4	5	6	7	8	9	10	11	12

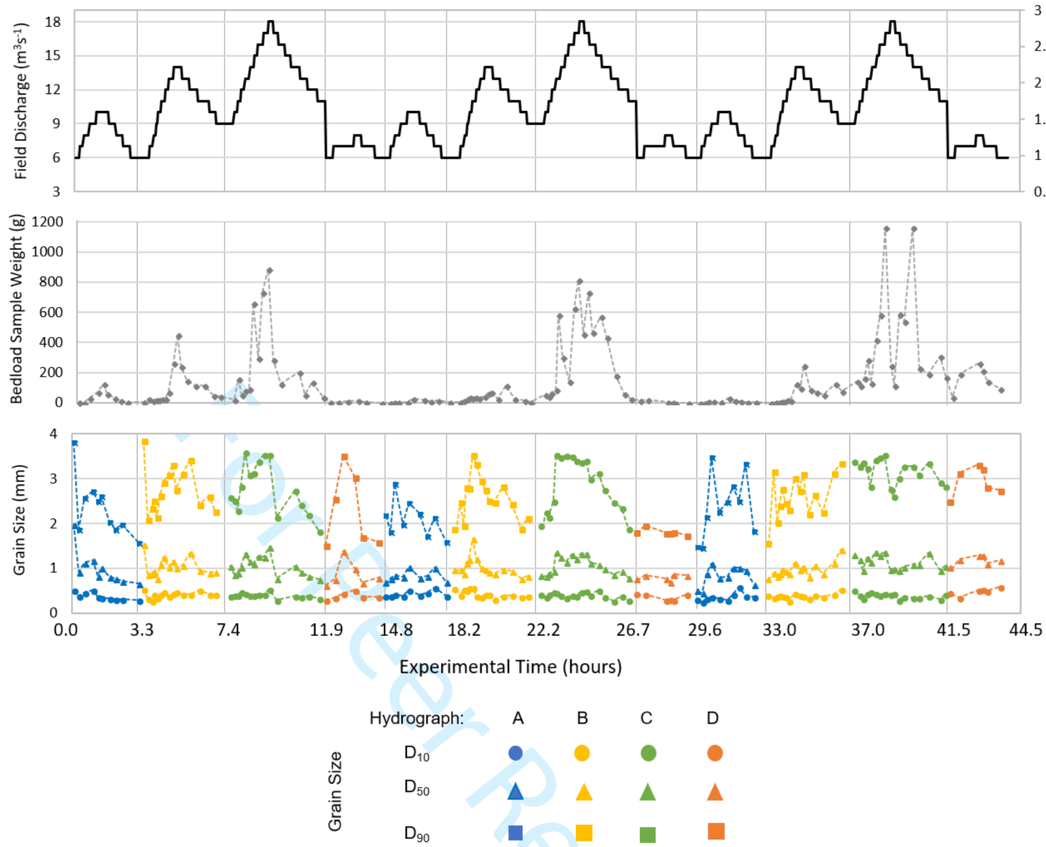

b)

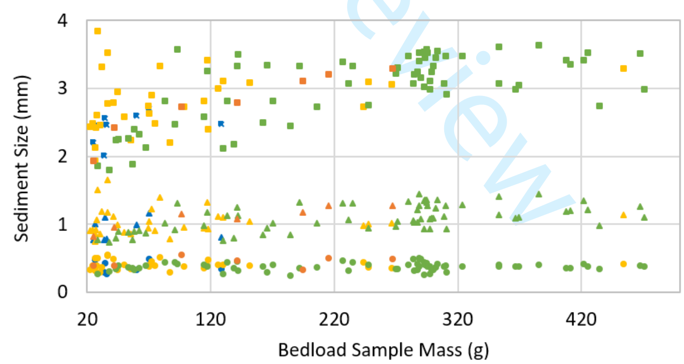

Figure 13 (a) The temporal relationship between bedload sample mass and grain size distribution throughout all hydrograph experimental runs. (b) The relationship between the mass of 1 minute bedload transport samples and the D_{10}, D_{50}, D_{90} of the sample.